Supplementary Methods

Transplant Strategy: This study used rhesus macaques that were housed at the Yerkes National Primate Research Center and at the Washington National Primate Research Center. Both FR104 and FR104/Sirolimus cohorts used half-sibling MHC haplo-identical donor and recipient pairs. Experiments were performed using our previously-described strategy for allogeneic HCT in rhesus macaques (1-4). Briefly, apheresis was performed after G-CSF mobilization (Amgen, 50mcg/kg for 5 days), and an unmanipulated apheresis product was transplanted into transplant recipients. The transplanted total nucleated cell dose (TNC) and CD3+ cell doses are shown in **Table 1**. The pre-HCT preparative regimen consisted of total body irradiation (TBI) of 10.4 cGy given in two fractions per day for two days. Irradiation was delivered with a Varian Clinac 23EX (Varian), at a dose rate of 7 cGy/min. All FR104/sirolimus recipients from the long-term cohort had a central venous catheter placed for the length of the experiment, and were given antibacterial prophylaxis which included vancomycin and ceftazidime. To investigate increases in WBC or neutrophil count, even without other clinical signs of infectious disease, both bacterial and fungal blood cultures were drawn, and further antibacterial agents were added as needed. Antiviral prophylaxis (acyclovir, 10 mg/kg IV daily; cidofovir, 5 mg/kg IV weekly) and antifungal prophylaxis (fluconazole 5mg/kg oral or IV, given daily) were also employed. Leukoreduced (using an LRF10 leukoreduction filter, Pall Medical) and irradiated (2200 rad) platelet-rich plasma or whole blood was given for a peripheral blood platelet count of $\leq 50 \times 10^3$ per μL or a hemoglobin < 9 g/dL, respectively, or if clinically significant hemorrhage was noted. Blood product support adhered to ABO antigen matching principles.

The aGVHD clinical score was assessed weekly for allo-HCT recipients as previously described (1-4). Briefly, the aGVHD clinical score increases with cumulative

GI-specific abnormalities (diarrhea), liver-specific abnormalities (hyperbilirubinemia) and skin-specific abnormalities (extent and character of rash). Statistical significance of the differences in clinical scores was determined using an unpaired t-test. It is important to note that the studies described focused on the natural history of aGVHD that developed during prophylaxis, such that animals were not given supplementary treatment when GVHD was diagnosed. Rather, when pre-defined clinical endpoints were met (based on the Emory and Washington National Primate Research Center veterinary standard operating procedures), animals were euthanized and a terminal analysis was performed. Thus, survival was directly related to the severity of clinical GVHD. Histopathologic scoring for GVHD was performed by an expert in GVHD histopathology (A.P.-M.) using a previously validated semi-quantitative scoring system (Grades 0.5-4)(1-4). The pathologist was blinded to the treatment cohorts during the scoring process. The Kaplan-Meier product-limit method was used to calculate survival. Differences between groups were determined using log-rank statistics.

Immunosuppressive regimens: Two FR104-containing prophylaxis cohorts were evaluated. In each cohort, recipients were prophylaxed with FR104 (sterile, endotoxin-free, as previously described (45, 46), purchased from Effimune/OSE Immunotherapeutics, Nantes, France) alone or in combination with Sirolimus (sirolimus was dosed once daily to attain a trough of 5-15 ng/ml as previously described(51, 52)). Animals received 5mg/kg of FR104 on days -1, +5, and then once a week thereafter until a pre-planned dosing endpoint for each of the FR104 cohorts (described below). The two cohorts were as follows: (1) A cohort of allogeneic transplant recipients receiving the anti-CD28 Fab' FR104 as monoprophylaxis ('FR104', n = 4, of which 1 (R.71) was a technical failure due to a failed apheresis procedure, leading to n = 3 for clinical and immune analysis, (recipient IDs R.22, R23 and R.24). Recipients in the mono-

prophylaxis cohort received weekly FR104 until they reached terminal analysis (median survival time (MST) = 21 days) (2) An allogeneic transplant cohort receiving dual prophylaxis with FR104 and Sirolimus ('FR104/Sirolimus', n = 9). This cohort consisted of 2 sub-groups (termed the 'short-term' (n= 4) and 'long-term' (n = 5) sub-groups) with pre-set experimental endpoints of 33-35 days and 100 days, respectively. In the short-term FR104/Sirolimus cohort, FR104 was dosed until the experimental endpoint. In the long-term cohort the dosing end-point occurred at Day +54. The short-term FR104/sirolimus cohort consisted of the following animals: R.26, R.27, R.28, R.29. The primary endpoint for this group was the proportion surviving to >33-35 days post-transplant. The range of 33-35 days was chosen to provide a window for necropsy scheduling. The long-term cohort consisted of the following animals: R.213, R.222, R.249, R.250, R.251. The primary endpoint for this cohort was the proportion surviving to >/=100 days. No treatment for aGVHD was provided to recipients in this study; therefore the clinical endpoints were unaffected by GVHD therapy.

The FR104 prophylaxis cohorts were compared to five additional cohorts, all of which have been previously described (12, 51, 52, 62). These included the following: (1) Autologous transplants (abbreviated as 'Auto', n = 6 for flow cytometric data and n = 4 for transcriptomic analysis); (2) An allogeneic transplant control cohort of recipients receiving no GVHD prophylaxis, ('No Rx', n = 11); (3) An allogeneic transplant cohort receiving Sirolimus mono-prophylaxis ('Sirolimus', n = 4); (4) An allogeneic transplant cohort receiving CTLA4-Ig as monotherapy for GVHD prophylaxis (abbreviated as 'CTLA4-Ig'. The belatacept formulation was used, which was supplied by Bristol Myers Squibb, n=4 for flow cytometry, n = 3 for transcriptomics); (5) An allogeneic transplant cohort receiving sirolimus (targeting a serum trough of 5-15 ng/dL) plus CTLA4-Ig for GVHD prophylaxis abbreviated 'CTLA4-Ig/Sirolimus' (n = 7).

Pharmacokinetics of FR104: Pharmacokinetic studies of FR104 were performed on

peripheral blood obtained longitudinally on FR104-treated recipients using ELISA as previously described (46).

CMV monitoring, Primary Prophylaxis and Treatment: Cytomegalovirus (CMV) monitoring was performed as previously described (5) and is reported as CMV copies/mL of whole blood. CMV viral load was measured twice weekly between days 0 to 30 post-HCT, then at lest once weekly from days 31 to 60 post-HCT and then at least once every 2 weeks thereafter. CMV prophylaxis and treatment was performed according to our standard NHP strategy, as previously described (6). Briefly, primary CMV prophylaxis was provided to all transplant recipients and included weekly cidofovir, given at a dose of 5mg/kg, along with renal protection with 3 doses of probenecid (167mg PO/dose) given within the first 24 hours after each cidofovir dose. Recipients who reactivated CMV continued cidofovir and were also treated with parenteral gancyclovir, which was given at 5mg/kg/dose twice daily. Gancyclovir treatment was continued until the serum copy number of CMV DNA was undetectable for two weeks and then discontinued.

Chimerism determination: Flow cytometrically-sorted T cells (CD3+/CD20-) were analyzed for donor chimerism based on divergent microsatellite markers. Chimerism analysis was performed at the UC Davis veterinary genetics laboratory as previously described (5).

Immune Analysis:

Measurement of serum cytokine concentrations: Serum cytokine concentrations were determined in serum samples using the 'Monkey 29-plex magnetic cytokine panel' or a custom-made 'Monkey 18-plex magnetic cytokine panel' (ThermoFisher Scientific) according to the manufacturer's instructions, and were measured using a Luminex 200

(Bio-Rad). Of these cytokines, 9 (Eotaxin, IFNγ, IL-1RA, IL-6, IL-12, I-TAC, MCP-1, MDC, MIF), were consistently 'in range' of detection, and so were chosen for full analysis.

Longitudinal Flow cytometry: Flow cytometric analysis was performed using the following gating strategy: First, cells were gated on FSC-A versus FSC-H and then on SSC-A versus SSC-H to discriminate doublets. Lymphocytes were then gated based on well-characterized FSC-A and SSC-A characteristics. The following phenotypic characteristics were then used to define immune cell populations: T cells: CD3+/CD14-/CD20- lymphocytes; CD4+ T cells: CD4+/CD3+/CD8-/CD14-/CD20- lymphocytes; CD8+ T cells: CD8+/CD3+/CD4-/CD14-/CD20- lymphocytes; Naïve CD4 or CD8 (T_N) T cells were determined as CD45RA+/CCR7+/CD95-. In addition, the expression of Granzyme B (GzmB) and Ki-67 were determined in CD8+ and CD4+ T cells. Relative percentages of each of these subpopulations were determined using FlowJo software (TreeStar) and absolute numbers of each of the subpopulations were determined by calculations from the complete blood count and absolute lymphocyte count analysis. To assess regulatory T cells PBMC were stained with extracellular antibodies (CD3, CD4, CD25, and CD127) followed by fixation/permeabilization with FoxP3 Fixation/Permeabilization kit (BioLegend) and staining with FoxP3 antibodies. Regulatory T cells were defined as CD25+CD127-FoxP3+ CD4 T cells. When staining was performed on thawed cells, LIVE/DEAD Aqua dye (Invitrogen) was used to discriminate viable cells from cell debris. The sources and clones used for each of the antibodies used in this study are shown in **Supplementary Table 9.**

Measuring CD28 expression on non-T cells:

Flow cytometric analysis was performed on freshly collected whole blood or bone marrow aspirate samples using the following gating strategy: First, cells were gated on

FSC-A versus FSC-H and then on SSC-A versus SSC-H to discriminate doublets. Lymphocytes, monocytes and granulocytes were then gated based on FSC-A and SSC-A parameters. The following phenotypic characteristics were then used to define immune cell populations: T cells: CD3+/CD20- lymphocytes; B cells: CD3-CD20+ lymphocytes; NK cells: CD8+CD16+CD3-CD20- lymphocytes; DC cells: HLA-DR+CD14-CD3-CD20- lymphocytes. Monocytes and granulocytes were first gated based on forward- and side-scatter. They were then gated on CD14+ cells (for monocytes) and CD11b+ cells (for granulocytes) to confirm their lineage. The indicated cell populations were then labeled with multiple anti-CD28 antibody clones, to rigorously determine if any expressed CD28 (antibodies listed in **Supplementary Table 9** and **Supplementary Figure** 2) as well as the corresponding isotype control IgGs. Intracellular CD28 expression was assessed after cells were fixed and permeabilized using Cytofix/Cytoperm reagents. For the detection of CD28 expression on platelets, whole blood samples were labeled with CD61 and CD28. After labeling, relative numbers of CD28-positive events within each cell populations were determined using FlowJo software (TreeStar). The sources and clones used for each of the antibodies used in this study are shown in **Supplementary Table 9.**

Allogeneic MLR assay to assess Treg suppressive function.

To determine whether in vitro exposure to FR104 impacted Treg suppressive function, CD25+ CD4 Treg cells were magnetically sorted from healthy immunologically naïve Rhesus macaques using the three-step sorting strategy. First, non-T cell fraction was selected using pan-T cell magnetic isolation kit for non-human primates LS magnetic column (Miltenyi Biotec), these cells were then irradiated (3500 cGy using ^{137}Cs source), labeled with 5 μM CellTracker Orange CMTMR (Invitrogen) and used for T cell stimulation ('Stimulator cells'). Second, the T cell-enriched flow-through fraction from the

first sorting step was then depleted from non-CD4 T cells, using biotinylated antibody cocktail from CD4+CD25+ Treg isolation kit and LS magnetic columns (Miltenyi Biotec). On-column fraction from this sorting step contains non-CD4 T cells. On the third step, the flow-through fraction from the previous sorting, enriched for CD4+ T cells, was positively selected for of CD25+ cells, using CD25-microbeads and MS columns (Miltenyi Biotec), resulting in selection of CD4+CD25+ T_{REG} cells (on column fraction) and CD4+CD25- flow-through fraction. The 'non-CD4 T cell' and 'CD4+ CD25- T cell' fractions from the same donor were then pooled together and referred to as the 'responder T_{CONV}' fraction. The responder Tconv were labeled with 5 μM CellTrace Violet (Invitrogen) and plated over stimulator cells from MHC-mismatched animal at a dose of $5x10^4$ cells/well in 96-well plates. CD25+ CD4 T cells (responder T_{REG}) were labeled with 5 μM CFSE (Invitrogen) and plated in various T_{CONV}:T_{REG} ratios (1:0; 8:1; 4:1; 2:1; 1:1). In some wells T_{REG} cells were pre-incubated with 10 μg/mL of FR104 for 1 hour and then washed before being plated, to assess the impact of exposure to FR104 on Treg function. Cells were then cultured for 6 days in X-VIVO 15 media (Lonza) supplemented with 10% FBS (ThermoFisher Scientific), 2 mM L-Glutamine (Invitrogen), penicillin/streptomycin (Invitrogen) and β-mercaptoethanol (Sigma). On day 6 cells were harvested, stained for CD3, CD4 and CD8 and for dead cells using 7-AAD and were acquired using FACSLSR Fortessa. The number of proliferating (CellTrace $Violet^{Lo}$) responder T_{CONV} was quantified using FlowJo software (TreeStar).

Flow cytometric assay for granulocyte-mediated phagocytosis and respiratory burst.

Whole blood from healthy human volunteers was collected into sodium citrate tubes, followed by red blood cell lysis using PharmLyse buffer (Becton Dickicnson). Resulting whole blood cells were pre-incubated for 1 hour with or without 10 μg/mL FR104 and then phagocytosis of E.Coli and the immune-complex-mediated respiratory burst were

measured using the pHrodo Red E.Coli BioParticle kit for flow cytometry (ThermoFisher Scientific) and using the Fc OxyBurst Green reagent (ThermoFisher Scientific), respectively, per manufacturer's instructions.

Flow Cytometric CD3+ T cell sorting and microarray cohort designation: Using a FACSAria or FACSJazz Cell Sorter (BD), T cells were sorted from 1) healthy controls, 2) autologous controls at day +14 and day +36, 3) allo-HCT recipients at day +14 post-transplant (as survival allowed), 4) allo-HCT recipients at day +28 post-transplant (as survival allowed) and 5) allo-HCT recipients at the time of terminal analysis. T cells were identified as CD3+/CD20- lymphocytes and were >90% pure based on post-sorting flow cytometric analysis as previously described (2). To prevent possible confounding that associated with graft failure/poor graft function in recipients in the long-term FR104/Sirolimus cohort, we excluded samples from recipients R.250 and R.251 (**Table 1**) that had lost donor chimerism or developed secondary graft failure, respectively, from transcriptomic analysis at all time points.

NHP Microarray and data analysis: Following T cell purification, RNA was stabilized in T cell lysates with RLT buffer (Qiagen) supplemented with 1% (vol/vol) beta-Mercaptoethanol (Sigma) and RNA was purified using RNEasy Column Kit (Qiagen). RNA was quantified using a Nanodrop Spectrophotometer (ThermoFisher Scientific) and purity was confirmed with an RNA 6000 Nano Kit (Agilent). The purified RNA was sent to the Vanderbilt Technologies for Advanced Genomics Core and to the Oregon Health Sciences University Gene Profiling Shared Resource where RNA quantity and quality were verified, followed by cDNA/cRNA synthesis, and target hybridization to GeneChip Rhesus Macaque Genome Array (Affymetrix). The resultant fluorescent signals were processed and normalized using the Robust Multichip Averaging (RMA) Method (7). The microarrays were performed in 5 batches, with all batches containing samples from both

healthy controls and transplanted animals. The "ComBat" algorithm was implemented to adjust for batch effects (8) and probe-sets containing low signal-to-noise measurement were filtered out in order to enhance statistical testing power(9). Probe-sets were annotated using 1) annotation file from Dr. Robert B. Norgren Jr.(10); 2) the annotation file provided by the chip manufacturer (release 33); and 3) data provided by Ingenuity Systems (Ingenuity Systems, www.ingenuity.com) for the small number of probe-sets that were not annotated by the chip manufacturer. Principal Component Analysis (PCA) was applied to summarize gene array variance using the Bioconductor MADE4 package (11). Analyses of gene differential expression (DE) was performed using an empirical Bayes moderated t-statistic, with a cutoff of 0.05, corrected for multiple hypothesis testing using Benjamini-Hochberg procedure and an absolute fold change cutoff > 1.4 with the limma package. Further analysis of differentiating characteristics of T cell transcriptional profiles involved Gene Set Enrichment Analysis (GSEA) using gene-sets from the Molecular Signatures Database v5.0 both on aggregate sample data from each cohort as a whole (8, 12, 13). In the current analysis, gene sets were ranked using a signal to noise ratio difference metric with 1000 permutations of gene set labels. Pathway analysis was performed using the DAVID 6.8 functional annotation tool (14). Class neighbor analysis was performed as previously described (15).

Network Analysis: Weighted gene coexpression network construction was performed as previously described (16). Briefly, the 4000 most variant genes were included in topologic overlap matrix construction. Soft thresholding power was chosen using scale free topology and a minimum module size of 50 was used to define modules. Further merging of modules was performed using a dynamic tree cut with a cut height of 0.25. Meta-modules were identified by clustering consensus module eigengenes with clinical characteristics. Visualization of WGCNA modules was performed using Cytoscape 3.0

using an edge threshold of 0.025 for the Blue module and 0.01 for the Brown module. Circular node layout was chosen to visualize networks. A false color scale denoting mean expression fold change was employed to visualize node expression data across clinical cohorts.

Supplementary Reference:

1. Furlan SN, Watkins B, Tkachev V, Cooley S, Panoskaltsis-Mortari A, Betz K, Brown M, Hunt DJ, Schell JB, Zeleski K, et al. Systems analysis uncovers inflammatory Th/Tc17-driven modules during acute GVHD in monkey and man. *Blood.* 2016.
2. Furlan SN, Watkins B, Tkachev V, Flynn R, Cooley S, Ramakrishnan S, Singh K, Giver C, Hamby K, Stempora L, et al. Transcriptome analysis of GVHD reveals aurora kinase A as a targetable pathway for disease prevention. *Sci Transl Med.* 2015;7(315):315ra191.
3. Miller WP, Srinivasan S, Panoskaltsis-Mortari A, Singh K, Sen S, Hamby K, Deane T, Stempora L, Beus J, Turner A, et al. GVHD after haploidentical transplantation: a novel, MHC-defined rhesus macaque model identifies CD28- CD8+ T cells as a reservoir of breakthrough T-cell proliferation during costimulation blockade and sirolimus-based immunosuppression. *Blood.* 2010;116(24):5403-18.
4. Tkachev V, Furlan SN, Watkins B, Hunt DJ, Zheng HB, Panoskaltsis-Mortari A, Betz K, Brown M, Schell JB, Zeleski K, et al. Combined OX40L and mTOR blockade controls effector T cell activation while preserving Treg reconstitution after transplant. *Sci Transl Med.* 2017;9(408).
5. Larsen CP, Page A, Linzie KH, Russell M, Deane T, Stempora L, Strobert E, Penedo MC, Ward T, Wiseman R, et al. An MHC-defined primate model reveals significant rejection of bone marrow after mixed chimerism

induction despite full MHC matching. *Am J Transplant.* 2010;10(11):2396-409.

6. Zheng HB, Watkins B, Tkachev V, Yu S, Tran D, Furlan S, Zeleski K, Singh K, Hamby K, Hotchkiss C, et al. The Knife's Edge of Tolerance: Inducing Stable Multilineage Mixed Chimerism but With a Significant Risk of CMV Reactivation and Disease in Rhesus Macaques. *Am J Transplant.* 2017;17(3):657-70.
7. Irizarry RA, Hobbs B, Collin F, Beazer-Barclay YD, Antonellis KJ, Scherf U, and Speed TP. Exploration, normalization, and summaries of high density oligonucleotide array probe level data. *Biostatistics.* 2003;4(2):249-64.
8. Johnson WE, Li C, and Rabinovic A. Adjusting batch effects in microarray expression data using empirical Bayes methods. *Biostatistics.* 2007;8(1):118-27.
9. Bourgon R, Gentleman R, and Huber W. Independent filtering increases detection power for high-throughput experiments. *Proc Natl Acad Sci U S A.* 2010;107(21):9546-51.
10. Duan F, Pauley MA, Spindel ER, Zhang L, and Norgren RB, Jr. Large scale analysis of positional effects of single-base mismatches on microarray gene expression data. *BioData Min.* 2010;3(1):2.
11. Culhane AC, Thioulouse J, Perriere G, and Higgins DG. MADE4: an R package for multivariate analysis of gene expression data. *Bioinformatics.* 2005;21(11):2789-90.

12. Mootha VK, Lindgren CM, Eriksson KF, Subramanian A, Sihag S, Lehar J, Puigserver P, Carlsson E, Ridderstrale M, Laurila E, et al. PGC-1alpha-responsive genes involved in oxidative phosphorylation are coordinately downregulated in human diabetes. *Nat Genet.* 2003;34(3):267-73.

13. Subramanian A, Tamayo P, Mootha VK, Mukherjee S, Ebert BL, Gillette MA, Paulovich A, Pomeroy SL, Golub TR, Lander ES, et al. Gene set enrichment analysis: a knowledge-based approach for interpreting genome-wide expression profiles. *Proc Natl Acad Sci U S A.* 2005;102(43):15545-50.

14. Huang da W, Sherman BT, and Lempicki RA. Systematic and integrative analysis of large gene lists using DAVID bioinformatics resources. *Nat Protoc.* 2009;4(1):44-57.

15. Golub TR, Slonim DK, Tamayo P, Huard C, Gaasenbeek M, Mesirov JP, Coller H, Loh ML, Downing JR, Caligiuri MA, et al. Molecular classification of cancer: class discovery and class prediction by gene expression monitoring. *Science.* 1999;286(5439):531-7.

16. Zhang B, and Horvath S. A general framework for weighted gene co-expression network analysis. *Stat Appl Genet Mol Biol.* 2005;4(Article17.

Supplementary Figure and Supplemetary Fugure Legend:

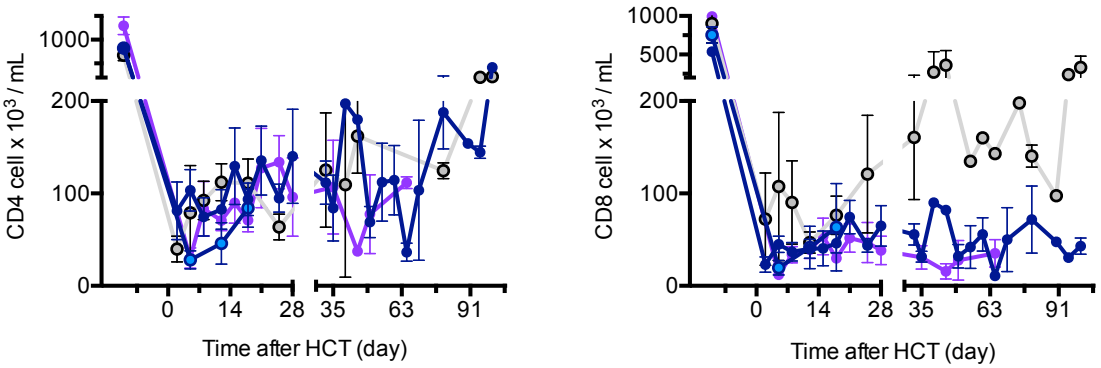

Supplementary Figure 1. **Impact of combinational GVHD immunoprophylaxis regimens on T cell reconstitution following HCT**. Absolute number of CD4 and CD8 T cells in the peripheral blood in the FR104/Sirolimus (*Blue*), CTLA4-Ig/Sirolimus (*Purple*) and Autologous (*Grey*) cohorts.

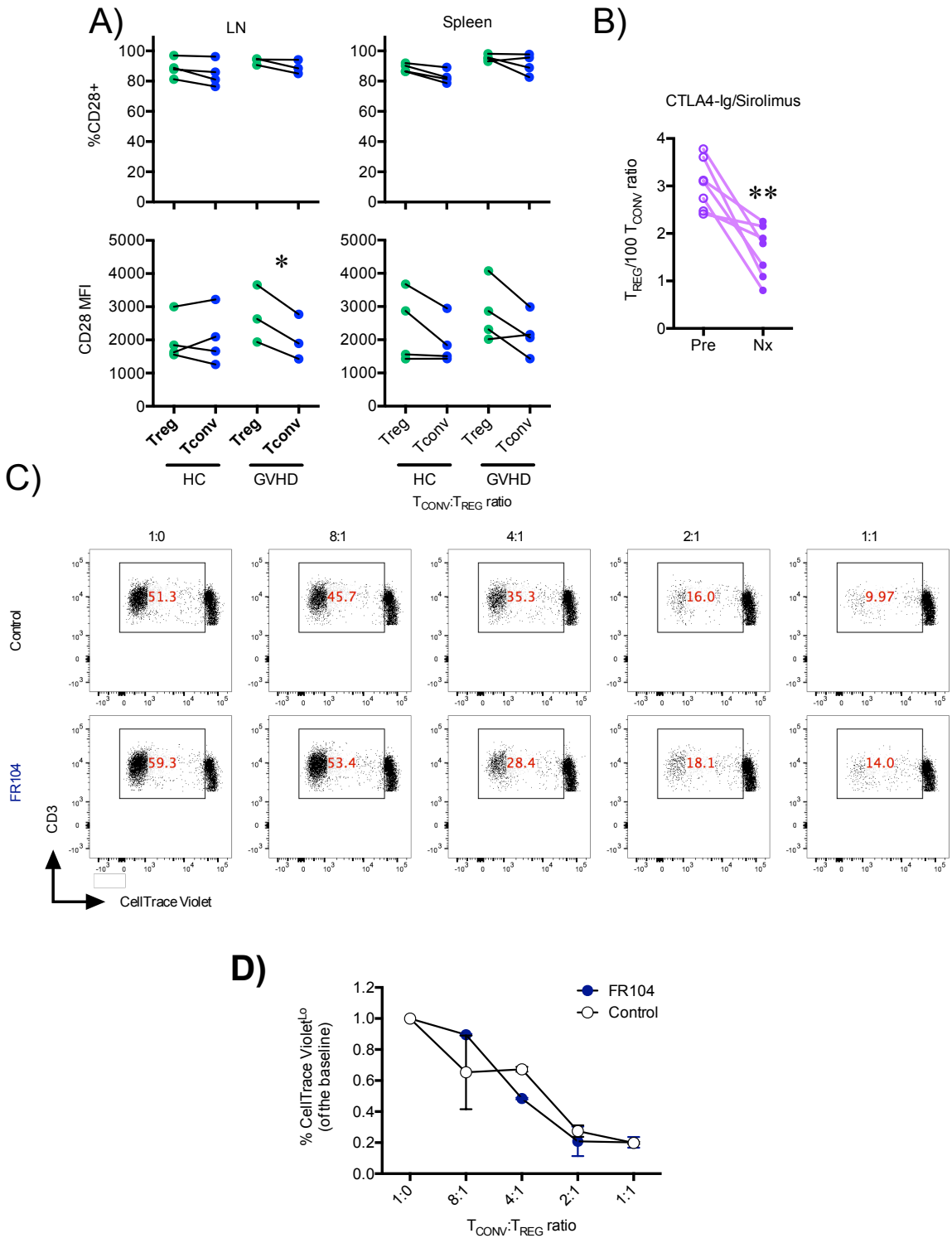

Supplementary Figure 2. **Impact of FR104 on T_{REG} reconstitution and function.** A) The relative number of CD28+ cells (*top panel*) and the relative level of CD28 expression in T_{REGs} (CD4+CD25+CD127- T cells) or in T_{CONV} (CD4+CD25-CD127+ T cells) populations. B) Treg:100 Tconv ratio in the peripheral blood in the CTLA4-Ig/Sirolimus cohort before HCT and at terminal analysis. C-D) Representative flow

cytometry plots depicting the percentage of prolifeating CD8+ T_{CONV} responder cells co-cultured with T_{REGs} in different ratios (C), and the resulting data from 2 donors presented as the proportion of CD8+ T_{CONV} responder cell proliferation normilized to the corresponding baseline (D).

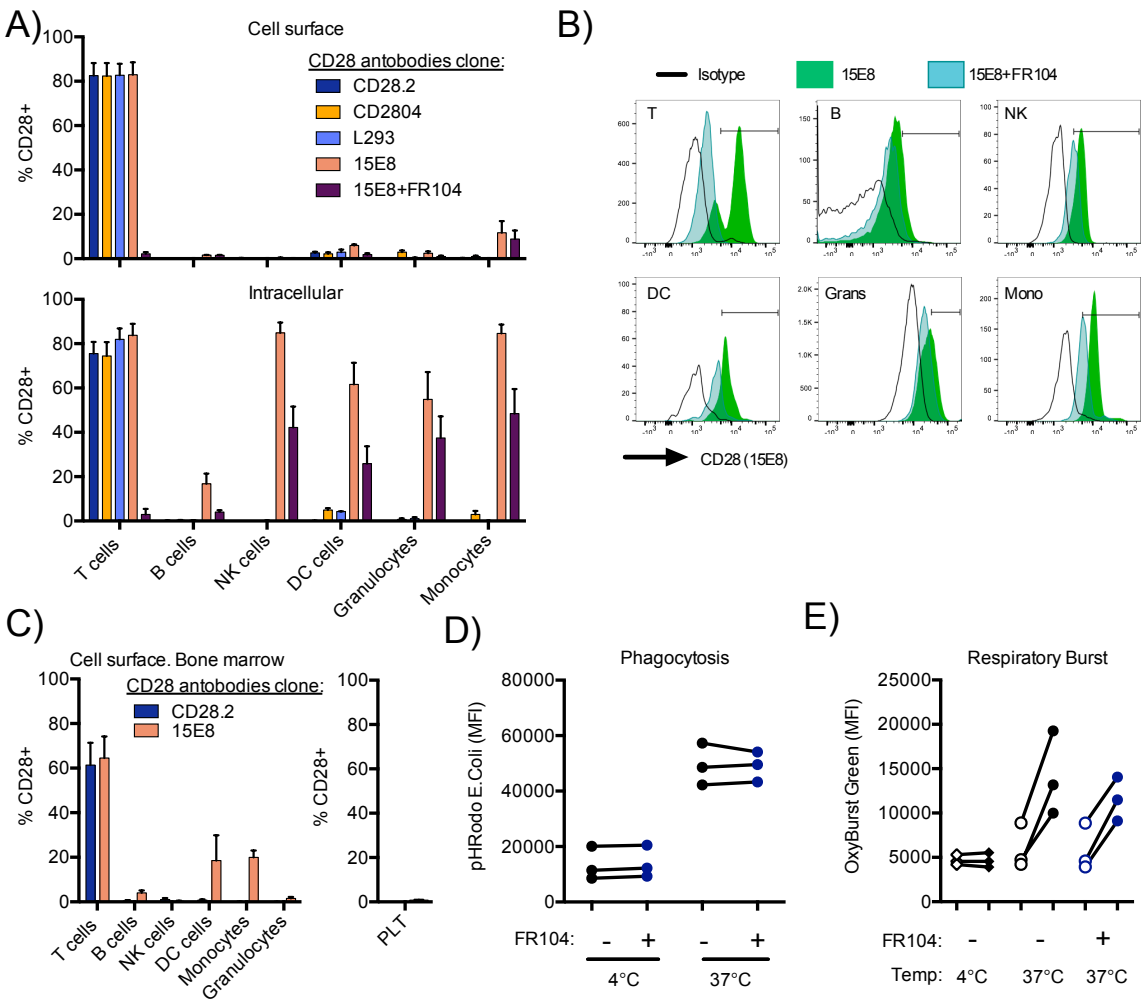

Supplementary Figure 3. **CD28 expression on non-T leukocytes and impact of FR104 on neutrophil function.** A) The relative number of cells expressing CD28 on the cell surface (*top panel*) or in the intracellular space (*bottom panel*). Staining on peripheral blood cells using four different anti-CD28 clones was performed as described in the **Supplementary methods**. B) Representative flowy cytometry plots showing intracellular staining of NHP leukocytes using anti-CD28 clone 15E8 antibodies with or withour pre-incubation with FR104. C) The relative number of NHP bone marrow cells (*left panel*) or blood platelets (*right panel*) expressing CD28 on the cell surface. D-E) Impact of short-term preincubation of whole blood cells with FR104 on *E.Coli* phagocytosis (D) or the respiratory burst (E) of granulocytes.

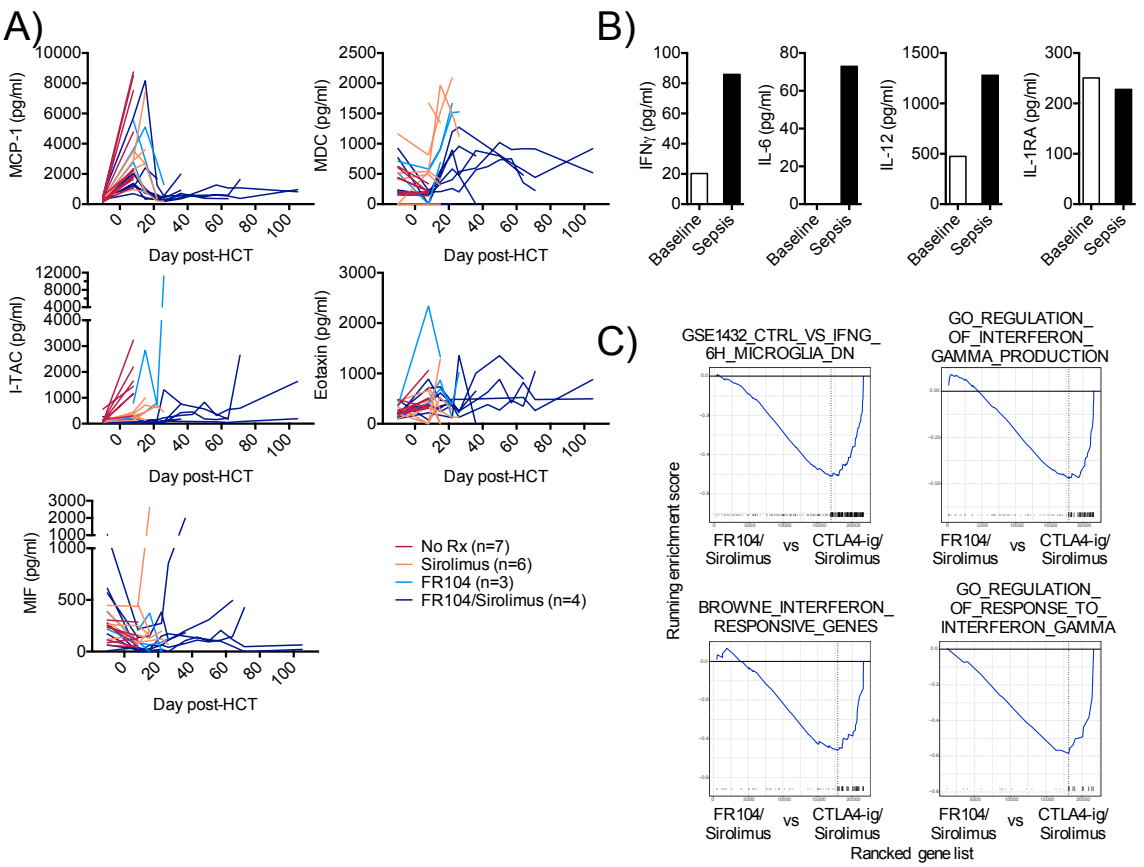

Supplementary Figure 4. **Serum cytokine and IFNγ GSEA analysis.**
A) Serum concentrations of pro-inflamatory cytokines (Eotaxin, I-TAC, MCP-1, MDC, MIF) in samples from recipients from the NoRx, Sirolimus, FR104 and FR104/Sirolimus cohorts. Each line represents a single transplant recipient.
B) Concentration of pro-inflamatory cytokines (IFNγ, IL-12, IL-6 and IL-1RA) in the serum of a control transplant recipient at baseline and during sepsis.
C) Representative IFNγ-related gene sets which were under-represented (using an FDR cut-off q<0.05) in the FR104/Sirolimus cohort in comparison with the CTLA4-Ig/Sirolimus cohort on day +14 post-HCT. The full list of gene sets over- or under-represented in FR104/Sirolimus cohort in comparison with CTLA4-Ig/sirolimus cohort is shown in **Supplementary Table 2**.

Supplementary Tables:

Supplementary Table 1. List of differentialy expressed (DE) genes between all experimental cohorts.
(see the corresponding excel file)

Supplementary Table 2. List of gene sets statistically over- or under-represented with q<0.05 in the FR104 and FR104/Sirolimus cohorts in comparison with other experimental groups.
(see the corresponding excel file)

Supplementary Table 3. Detailed histopathology scores for the FR104/Sirolimus cohort.

FR104/Sirolimus cohort <D66				FR104/Sirolimus cohort >D66			
Animal ID	Skin	Liver	Colon	Animal ID	Skin	Liver	Colon
R.26	1	0.5	Not calculated*	R.249	0.5	1.5	0.5
R.27	0.5	1.5	Not calculated*	R.250	1.5	1.5	2
R.28	1	1.5	2	R.251	1.5	1.5	2
R.29	0.5	0.5	1				
R.213	1	0	Not calculated*				
R.222	0	1.5	2				

***Not included in the combined histopathology score due to documented GI Infection**

Supplementary Table 4. List of DE genes shown in Figure 5A-B.
(see the corresponding excel file)

Supplementary Table 5. Pathway analysis of DE genes shown in Figure 5C.
(see the corresponding excel file)

Supplementary Table 6. Transcripts lists of gene modules resulting from WCGNA performed on transcriptomes from the HC, No Rx, FR104/Sirolimus and CTLA4-Ig/Sirolimus cohorts.
(see the corresponding excel file)

Supplementary Table 7. Pathway analysis of genes from Blue module.
(see the corresponding excel file)

Supplementary Table 8. MHC-matching characteristics of the transplants included in the current study.

Cohort	Animal ID	Role in transplant	MHC typing						Relationship and Matching
No prophylaxis	R.16	Donor	A002a	A004	B012a	B028	DR03f	DR14a	Half-sibs, Haplo-identical
	R.50	Recipient	A004	A001	B028	B047a	DR14a	DR03a	
No prophylaxis	R.36	Donor	A004	A008	B012b	B024a	[DR04a]	DR13a	Unrelated, MHC mismatched
	R.51	Recipient	A004	A001	B001a	B047a	DR04a	DR04a	
No prophylaxis	R.58	Donor	A001	A006	B017a	B069a	DR04a	DR01a	Half-sibs, Haplo-identical
	R.52	Recipient	A001	A004	B017a	B012b	DR03a	DR01a	
No prophylaxis	R.59	Donor	A008	A004	B012b	B028	DR03a	DR09a	Unrelated, Haplo-identical
	R.53	Recipient	A008	A016	B001b	B028	[DR04a]	?	
No prophylaxis	R.222	Donor	A052	A019	B003a	*B039a*	*DR03f*	DR-unkn1	Half-sibs, haplo-identical
	R.229	Recipient	A052	A026	B003a	*B056b*	*DR03f*	DR-unkn	
No prophylaxis	R.223	Donor	A004	A002a	B002	B012a	DR06	DR03f	Unrelated, haplo-identical
	R.230	Recipient	A001	A002a	B047a	B012a	DR04a	DR16	
No prophylaxis	R.224	Donor	A001	A002a	B055	B015a	DR03g	DR15a	Unrelated, haplo-identical
	R.231	Recipient	A001	A019	B055	B015c	DR03g	DR03a	
No prophylaxis	R.225	Donor	A004	A004	B012b	B002	DR04a	DR06	Unrelated, haplo-identical
	R.232	Recipient	A004	A001	B012b	B055	DR04a	DR03g	
No prophylaxis	R.226	Donor	A008	A004	B069b	*B015a*	*DR04a*	DR16	Half-sibs, haplo-identical
	R.233	Recipient	A008	A019	B069b	*B015c*	*DR04a*	DR03a	
No prophylaxis	R.227	Donor	A026	A008	B012a	*B106*	DR04a	DR11a	Half-sibs, haplo-identical
	R.234	Recipient	A026	A007	B012a	B077a	DR04a	DR02b	
No prophylaxis	R.228	Donor	A026	A004	B012a	*B069b*	DR04a	DR06	Half-sibs, haplo-identical
	R.235	Recipient	A026	A008	B012a	B015a	DR04a	DR01a	
CTLA4-Ig	R.45	Donor	A002a	A004	B012a	B012a	DR03f	DR11a	Unrelated, Haplo-identical
	R.46	Recipient	A002a	A224a	B012a	B029	DR03f	DR04a	
CTLA4-Ig	R.48	Donor	A085	A052	B010a	B025a	DR09c	DR03j	Half-sibs, MHC mismathed
	R.47	Recipient	A085	A052	B001a'	B056d	DR26	DR29	
CTLA4-Ig	R.49	Donor	A018b	A002a'	B001a'	B002	DR17b	DR14c	Unrelated, MHC mismatched
	R.54	Recipient	A049	A004	B017g	B106	DR06b	DR13c	
CTLA4-Ig	R.56	Donor	A018a	A056a	B015d	B069a'	DR16	recDR14/15	Half-sibs, Haplo-identical
	R.57	Recipient	A018a	A074	B015d	[B039a]	DR16	[DR08]	
Sirolimus	R.32	Donor	A008	A004	B069b	B056b	DR04a	DR03a	Half-sibs, Haplo-identical
	R.13	Recipient	A008	A019b	B069b	B015c	DR04a	DR03a	
Sirolimus	R.37	Donor	A002a	A004	B001c	B012b	DR15a/b	DR04a	Unrelated, MHC mismatched
	R.16	Recipient	A002a	A004	B012a	B028	DR03f	DR14a	
Sirolimus	R.63	Donor	A002a	A004	B012a	B056b	DR03f	DR15a/b	Half-sibs, MHC-mismathed
	R.17	Recipient	A110/A111	A004	B043b	B015a	DR14b	DR04a	
Sirolimus	R.33	Donor	A004	A007	B012b	B012b	DR04a	DR03a	Half-sibs, Haplo-identical
	R.18	Recipient	A004	A004	B012b	B069a	DR04a	DR03a	
CTLA4-Ig/Sirolimus	R.39	Donor	A006	A001	B043a	B017a	DR03f	DR03a	Half-sibs, Haplo-identical

	R.38	Recipient	A006	A008	B043a	B069a	DR03f	DR03h	
CTLA4-Ig/Sirolimus	R.31	Donor	A019b	A049	B015c	B071	DR03a	DR01a	Half-sibs, Haplo-identical
	R.42	Recipient	A002a	A049	B012a	B071	DR03f	DR01a	
CTLA4-Ig/Sirolimus	R.56	Donor	A018a	A056a	B015d	B069a'	DR16	recDR14/15	Unrelated, MHC mismatched
	R.49	Recipient	A018b	A002a'	B001a'	B002	DR17b	DR14c	
CTLA4-Ig/Sirolimus	R.54	Donor	A049	A004	B017g	B106	DR06b	DR13c	Half-sibs, Haplo-identical
	R.66	Recipient	A049	A019	B017g	B013a	DR06b	DR27c	
CTLA4-Ig/Sirolimus	R.48	Donor	A085	A052	B010a	B025a	DR09c	DR03j	Half-sibs, Haplo-identical
	R.67	Recipient	A085	A019	B010a	B101	DR09c	DR27b	
CTLA4-Ig/Sirolimus	R.47	Donor	A085	A052	B001a'	B056d	DR26	DR29	Half-sibs, Haplo-identical
	R.68	Recipient	A085	A122	B001a'	B077a	DR26	DR26	
CTLA4-Ig/Sirolimus	R.49	Donor	A018b	A002a'	B001a'	B002	DR17b	DR14c	Half-sibs, Haplo-identical
	R.70	Recipient	A018b	A003	B001a'	B004	DR17b	DR11a	
FR104	R.264	Donor	A006	A004	B008	B012b	DR03c	DR03a	Half-sibs, Haplo-identical
	R.22	Recipient	A006	A110	B008	B043b	DR03c	DR14b	
FR104	R.265	Donor	A105	A008	B002	B048	DR-unk3	DR15a/b	Half-sibs, Haplo-identical
	R.23	Recipient	A002a	A008	B012a	B048	DR16	DR15a/b	
FR104	R.55	Donor	A006	A008	B008	B012b	DR03c	DR03a	Unrelated, MHC mismatched
	R.24	Recipient	A019	A049	B015c	B071	DR1a	DR11a	
FR104/Siro	R.266	Donor	A002a	A025	B015a	B017a	DR15a/b	DR16	Half-sibs, Haplo-identical
	R.26	Recipient	A002a	A004	B015a	B001a	DR15a/b	DR06	
FR104/Siro	R.22	Donor	A006	A110	B008	B043b	DR03c	DR14b	Half-sibs, Haplo-identical
	R.27	Recipient	A006	A004	B008	B048	DR03c	DR01a	
FR104/Siro	R.55	Donor	A006	A008	B008	B012b	DR03c	DR03a	Half-sibs, Haplo-identical
	R.28	Recipient	A006	A004	B008	B001a	DR03c	DR04a	
FR104/Siro	R.41	Donor	A002a	A004	B012a	B012a	DR03f	DR11a	Half-sibs, Haplo-identical
	R.29	Recipient	A002a	A224a	B012a	B029	DR03f	DR04a	
FR104/Siro	R.208	Donor	A023	A019	B012b	B017a	DR03f	DR10a	Unrelated, MHC mismatched
	R.222	Recipient	A052	A019	B003a	B039a	DR03f	DR-unk1	
FR104/Siro	R.253	Donor	A006	A002a	B069a	B069a	DR-unk	DR-unk	Half-sibs, Haplo-identical
	R.249	Recipient	A006	A028	B069a	B001a	DR04a	DR11a	
FR104/Siro	R.254	Donor	A019	A008	B015c	B069b	DR03a	DR04a	Full sibs, Haplo-identical
	R.213	Recipient	A019	A105	B015c	B048	DR03a	DR-unk	
FR104/Siro	R.254	Donor	A019	A008	B015c	B069b	DR03a	DR04a	Half-sibs, Haplo-identical
	R.250	Recipient	A019	A002a	B015c	B012a	DR03a	DR03f	
FR104/Siro	R.216	Donor	A074	A004	B001a	B012b	DR13a	DR04a	Half-sibs, Haplo-identical
	R.251	Recipient	A074	A023	B001a	B055	DR13a	DR01c	

Supplementary Table 9. List of flow cytometry reagents used in the current study.

Marker	Clone	Vendor
CCR7	G043H7	Biolegend
CD127	eBioRDR5	eBioscience
CD14	M5E2	BD Biosciences
CD20	2H7	eBioscience
CD25	4E3	Miltenyi Biotech
CD28	CD28.2	eBioscience
CD3	SP34-2	BD Biosciences
CD4	L200	BD Biosciences
CD45RA	2H4LDH11LDB9	Beckman Coulter
CD8	RPA-T8	BD Biosciences
CD95	DX2	Biolegend
Ki-67	Ki-67	Dako
Granzyme B	FGB12	Invitrogen
FoxP3	20D6	Biolegend
FoxP3	259D/C7	BD Biosciences
CD16	3G8	BD Biosciences
CD11b	ICRF44	BD Biosciences
HLA-DR	G46-6	BD Biosciences
CD28	L246	BD Biosciences
CD28	CD2804	Invitrogen
CD28	15E8	Miltenyi Biotech
CD61	Y2/51	Miltenyi Biotech